Weakened rate-dependent depression of Hoffmann's reflex and increased motoneuron hyperactivity after motor cortical infarction in mice

S Lee*,[1], T Toda[1], H Kiyama[2] and T Yamashita[3]

Abnormal reflexes associated with spasticity are considered a major determinant of motor impairments occurring after stroke; however, the mechanisms underlying post-stroke spasticity remain unclear. This may be because of the lack of suitable rodent models for studying spasticity after cortical injuries. Thus, the purpose of the present study was to establish an appropriate post-stroke spasticity mouse model. We induced photothrombotic injury in the rostral and caudal forelimb motor areas of mice and used the rate-dependent depression (RDD) of Hoffmann's reflex (H-reflex) as an indicator of spastic symptoms. To detect motoneuron excitability, we examined c-fos mRNA levels and c-Fos immunoreactivity in affected motoneurons using quantitative real-time reverse transcription PCR and immunohistochemical analysis, respectively. To confirm the validity of our model, we confirmed the effect of the anti-spasticity drug baclofen on H-reflex RDDs 1 week post stroke. We found that 3 days after stroke, the RDD was significantly weakened in the affected muscles of stroke mice compared with sham-operated mice, and this was observed for 8 weeks. The c-fos mRNA levels in affected motoneurons were significantly increased in stroke mice compared with sham-operated mice. Immunohistochemical analysis revealed a significant increase in the number of c-Fos-positive motoneurons in stroke mice compared with sham-operated mice at 1, 2, 4, and 8 weeks after stroke; however, the number of c-Fos-positive motoneurons on both sides of the brain gradually decreased over time. Baclofen treatment resulted in recovery of the weakened RDD at 1 week post stroke. Our findings suggest that this is a viable animal model of post-stroke spasticity.

Spasticity is common in patients with brain and spinal cord injuries.[1,2] Approximately 20–40% of patients with stroke exhibit spasticity,[3–5] whereby neurological damage disrupts voluntary movement control. Consequently, these patients' quality of life is significantly lower compared with that of patients without post-stroke spasticity.[6]

A velocity-dependent increase in muscle tone resulting from stretch reflex hyperexcitability has been proposed as a cardinal feature of spasticity.[7,8] In addition, spinal reflex spasticity is known to be accompanied by weakened rate-dependent depression (RDD) of Hoffmann's reflex (H-reflex), which is the electrical analog of the tendon jerk reflex and is mediated through monosynaptic pathways in the spinal cord. Electromyograms recorded during H-reflexes typically display two responses: an initial M wave, which is the result of direct activation of motor axons, and an H-reflex, which is elicited by the synaptic activation of motoneurons. The RDD of the H-reflex refers to the phenomenon by which the magnitude of the H-reflex is temporarily attenuated by repetitive stimulation. Given that

spasticity develops in conjunction with weakening RDD of the H-reflex, which is gradually abolished following brain and spinal cord injury, RDD is considered a reliable measurement of spasticity in stroke patients and in animal models of spinal cord injury.[9–11]

It is clear that stroke can cause inhibitory and excitatory impulse imbalance, leading to upper motoneuron symptoms, and it is known that lesion location and extent can result in differing symptoms and degrees of spasticity severity; however, the pathophysiological basis of spasticity remains poorly understood.[12] It is accepted that spasticity involves over-reactivity of alpha motoneurons and alterations in primary Ia reciprocal inhibition and Renshaw recurrent inhibition,[13–17] but further understanding of the underlying mechanisms is hindered by the lack of animal models. In one study, Fulton and Kennard[18] used primates to demonstrate that lesions in both primary and premotor areas can induce spasticity; however, a rodent model is needed to analyze the precise mechanisms underlying spasticity after cortical injuries, such as those in stroke.

[1]Department of Rehabilitation Sciences, Graduate School of Medicine, Nagoya University, 1-1-20 Daiko-minami Higashi-ku, Nagoya-shi, Aichi, Japan; [2]Department of Functional Anatomy and Neuroscience, Graduate School of Medicine, Nagoya University, 65 Tsurumai-tyou Shouwa-ku, Nagoya-shi, Aichi, Japan and [3]Department of Molecular Neuroscience, Graduate School of Medicine, Osaka University, 2-2 Yamadaoka, Suita-shi, Osaka, Japan
*Corresponding author: S Lee, Department of Rehabilitation Sciences, Graduate School of Medicine, Nagoya University, 1-1-20 Daiko-minami Higashi-ku, Nagoya-shi, Nagoya 461-8673, Japan. Tel: +81 52 719 1365; Fax: +81 52 719 1365; E-mail: lee@met.nagoya-u.ac.jp
Keywords: Stroke; spasticity; mouse
Abbreviations: RDD, rate-dependent depression; H-reflex, Hoffmann's reflex; PFA, paraformaldehyde; PBS, phosphate-buffered saline; LMD, laser microdissection; RT-PCR, reverse transcription-PCR; ChAT, choline acetyltransferase; GAPDH, glyceraldehyde-3-phosphate dehydrogenase; ANOVA, analysis of variance; GABA, gamma-aminobutyric acid
Received 26.8.13; revised 04.12.13; accepted 09.12.13; Edited by A Verkhratsky

Here, we investigated whether spasticity is induced after photothrombotic injury to the rostral and caudal forelimb motor areas of mice, which are considered the premotor and forelimb primary motor cortices in rodents, respectively.[19] Given that enhanced excitability of affected motoneurons has frequently been reported in studies of spasticity after stroke and spinal cord injury, we further examined whether a similar phenomenon occurred in our mouse model of post-stroke spasticity.

Results

Location and volume of cortical infarct lesions. We unilaterally induced focal thrombotic stroke to the rostral and caudal forelimb motor areas of mice using the Rose Bengal photothrombotic method.[20–22] Lesions in the rostral and caudal forelimb motor areas were reproducible (Figures 1a and b). Nissl-stained coronal sections from the lesioned areas obtained 8 weeks after stroke demonstrated neuronal loss in the infarcted area, and volume quantification demonstrated that the lesion was $2.56 \pm 0.28 \, mm^3$ ($n = 5$) in size.[22]

Reduction of H-reflex RDD after stroke. To test whether an affected muscle exhibited spastic symptoms after stroke, we measured H-reflex RDDs in the affected and unaffected abductor digiti minimi muscles 3 days and 1, 2, 3, 4, 6, and 8 weeks after stroke. The H-reflex magnitudes were attenuated by repeated activations at frequencies $> 0.1 \, Hz$. In particular, we observed a reduction of $> 80\%$ of the H-reflex magnitude at 5 Hz in sham-operated mice (Figure 2a, upper panel). In contrast, the H-reflex magnitude in 4-week stroke mice was not strongly attenuated by repeated activation (Figure 2a, lower panel). Moreover, we found that RDDs for the affected muscles were significantly weakened in stroke mice ($n = 6$) compared with sham-operated mice ($n = 7$) 3 days after stroke, and this was still observed on week 8 after stroke ($P < 0.01$, Figure 2b); however, the RDDs were not significantly weakened at week 3. In addition, the RDDs of stroke mice were significantly smaller at week 6 than at weeks 4 and 8 ($P < 0.01$). Four weeks after stroke, the RDDs induced at all frequencies $> 0.1 \, Hz$ were significantly smaller in stroke mice than in sham-operated mice (Figure 2c). This indicates that the affected muscles exhibited spastic post-stroke symptoms in our model.

In addition, we compared H-reflex RDDs elicited by 5 Hz in the unaffected muscles of the sham-operated and stroke mice (Figure 2d). We found that at weeks 1 and 8, the RDDs in the unaffected muscles were significantly smaller in stroke mice compared with sham-operated mice ($P < 0.01$ for week 1 and $P < 0.05$ for week 8); this suggests that the RDDs in the unaffected muscles were also influenced by cortical injuries. However, it should be noted that the RDDs of sham-operated and stroke mice were not significantly different at any other time point in the unaffected muscles (Figure 2d).

Similarly, we compared the RDDs at 5 Hz for the affected and unaffected muscles of stroke and sham-operated mice separately (Figures 3a and b). In stroke mice, the RDDs for the affected side were significantly smaller than those for the unaffected side at 1, 2, 3, and 6 weeks after stroke ($P < 0.01$ for 1, 2, and 6 weeks and $P < 0.05$ for 3 weeks; Figure 3a); however, the weakened depressions at 4 and 8 weeks were not significantly different between the two sides. In contrast, there were no differences in the RDDs between the affected and unaffected sides of sham-operated mice (Figure 3b).

We also examined RDDs in the abductor pollicis brevis muscles after stroke and found that at 1 week after stroke they were significantly smaller in stroke mice compared with sham-operated mice ($P < 0.01$, data not shown). These results indicate that some muscles developed spastic symptoms after cortical injury in this model system.

Motoneuron hyperactivation after stroke. It has been reported that one of the mechanisms underlying spasticity in stroke patients is increased neuronal excitability of the
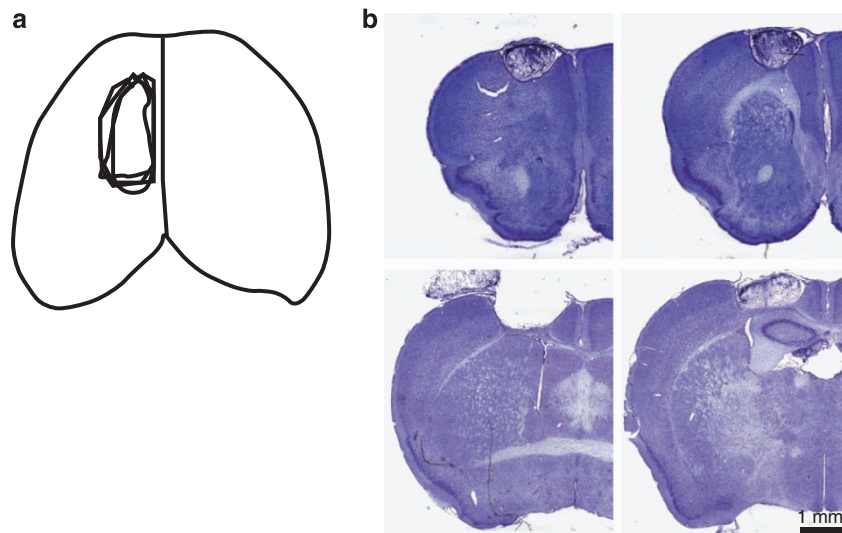
Figure 1 (**a**) Schematic representation showing the lesion areas ($n = 4$). These hemicortical lesions were reproducible. (**b**) Coronal sections of Nissl-stained injured brain; specifically, the rostral and caudal forelimb areas were injured (Nissl staining)
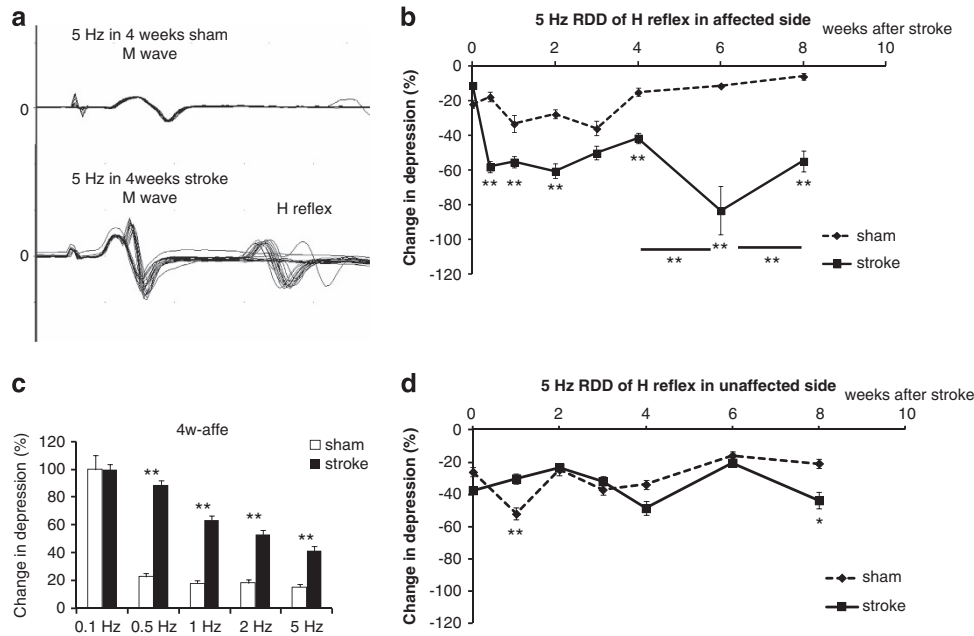
Figure 2 RDD of H-reflex in sham-operated and stroke mice. (**a**) Repeated stimulation at 5 Hz weakened H-reflex amplitude in normal mice (upper). In stroke mice, H-reflex was not weakened upon repeated stimulation at 5 Hz (lower). (**b**) Changes in H-reflex depression (%) with 5-Hz stimulation on the affected side in stoke and sham-operated mice. (**c**) H-reflex RDD 4 weeks after stroke. Response data are expressed as percentages relative to the mean responses at 0.1 Hz in the same series of measurements. (**d**) Changes in H-reflex depression (%) with stimulation at 5 Hz on the unaffected side in stroke and in sham-operated mice. (sham-operated group, dotted line; stroke group, solid line) Data are shown as the mean ± S.E.M. *$P < 0.05$, **$P < 0.01$ ($n = 7$ for sham-operated mice and $n = 6$ for stroke mice, one-way ANOVA followed by Tukey–Kramer tests)

propriospinal neurons and motoneurons.[14,17,23] To determine whether motoneuron excitability was increased after stroke, we performed quantitative real-time reverse transcription PCR (RT-PCR) to examine the gene expression of c-fos, an activity-dependent immediate early gene, in spinal motoneurons.[24,25] A retrograde tracer and laser microdissection (LMD) technique was used to obtain affected motoneurons (Figure 4A). Expression of c-fos mRNA in the affected neurons was significantly increased for stroke mice ($n = 3$) compared with sham-operated mice ($n = 4$) (~50 neurons from each mouse were analyzed; Mann–Whitney U test, $P < 0.01$, Figure 4B).

Furthermore, we measured c-Fos immunoreactivity in motoneurons labeled for choline acetyltransferase (ChAT) using spinal sections from the cervical to the thoracic level (C4–T1) obtained 1, 2, 4, and 8 weeks after stroke. At 1 week after stroke, c-Fos induction in the affected and unaffected neurons was significantly increased in stroke mice compared with sham-operated mice at most spinal levels ($n = 3$ for groups; **$P < 0.01$, in C4–T1, compared between sham-operated and stroke mice on the affected side; #$P < 0.05$ in C4, ##$P < 0.01$, in C6–T1, compared between sham-operated and stroke mice on the unaffected side; Figures 4c and d). Moreover, at 2 weeks after stroke, the number of c-Fos-positive motoneurons at C4–T1 of stroke mice significantly increased on the affected side compared with the affected side of the sham-operated mice ($n = 3$ for groups; *$P < 0.05$, Figure 4E). Similarly, at 4 weeks after stroke, the number of c-Fos-positive motoneurons in the affected side of stroke mice significantly increased compared with the affected side of the sham-operated mice at C4–C7 ($n = 3$ for groups; **$P < 0.01$ in

C4–C7; Figure 4F). At 8 weeks after stroke, the number of c-Fos-positive neurons at C7 and T1 on the affected side was significantly higher in stroke mice compared with sham-operated mice ($n = 3$ for groups; *$P < 0.05$; 8 weeks in C7 and T1; Figure 4G); however, stroke mice showed a gradual decrease in this number during the eighth week after stroke (C4; $r = -0.33$, $P < 0.01$, C5; $r = -0.31$, $P < 0.01$, C6; $r = -0.39$, $P < 0.01$, C7; $r = -0.32$, $P < 0.01$, T1; $r = -0.48$, $P < 0.01$; Figure 5a). In the unaffected side in stroke mice, we observed a similar increase in the number of c-Fos-positive neurons (C6; $r = -0.41$, $P < 0.01$, C7; $r = -0.46$, $P < 0.01$, T1; $r = -0.30$, $P < 0.01$; Figure 5b).

In addition, compared with the unaffected side of stroke mice, their affected side showed significantly increased number of c-Fos-positive motoneurons at C4 and C5 on week 1 and at C6 on week 4 after stroke (††$P < 0.01$ at 1 week; †$P < 0.05$ at 4 weeks; Figures 4d and f). These results suggest that the motoneurons, which innervate both the affected and unaffected muscles, were excited.

Effective spasticity suppression with baclofen. Many clinical and experimental animal pharmacology studies have used the anti-spasticity agent baclofen, which is a gamma-aminobutyric acid (GABA)$_B$ receptor agonist.[26,27] To confirm whether spastic symptoms, such as weakened RDD, were inhibited following administration of an anti-spasticity agent, we measured H-reflex RDD in mice intraperitoneally injected with baclofen at 1 week after stroke. The mice, which exhibited weakened RDD at 3 days after stroke (Figure 6a), were injected with baclofen or 0.9% NaCl as vehicle before H-reflex RDD measurement. We found that weakened RDDs

a

5 Hz RDD of H reflex in stroke

b

5 Hz RDD of H reflex in sham
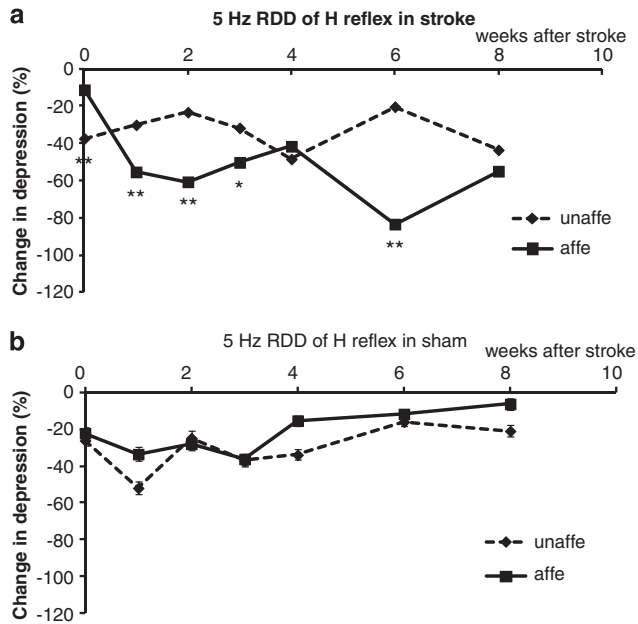
Figure 3 RDDs of H-reflexes of the affected and unaffected sides in (**a**) stroke and (**b**) sham-operated mice. Data are represented as the mean ± S.E.M. *$P < 0.05$, **$P < 0.01$ ($n = 7$ for sham-operated mice and $n = 6$ for stroke mice, one-way ANOVA followed by Tukey–Kramer tests)

were significantly recovered in baclofen-injected stroke mice ($n = 5$) compared with vehicle-injected stroke mice ($n = 4$, $P < 0.01$; Figure 6b).

We also examined RDDs in baclofen-injected intact mice and found that RDDs were not significantly different from those in vehicle-injected intact mice (data not shown).

Discussion

Spasticity is a common complication after stroke; however, the underlying pathophysiology remains unclear, and research into this area is hampered by the lack of appropriate animal models. The present study reveals that lesions in the rostral and caudal forelimb motor areas of the mouse brain induce spasticity, as indicated by weakened H-reflex RDDs, increased motoneuron excitability of affected muscles and recovered RDDs in stroke mice following baclofen treatment. Our findings raise the possibility that this protocol may yield a viable animal model of post-stroke spasticity.

Clinically, increased muscle tone (i.e., an increase in resistance to passive stretch) occurs because of increased reflex activity and intrinsic changes in the muscles.[3] Reflex-mediated increases in patient muscle tone reach a maximum between 1 and 3 months after stroke,[3,28] and it has been proposed that after 3 months, the increased resistance to passive stretch is attributable to intrinsic changes in the muscles.[28] We found that the weakened H-reflex RDDs exhibited two phases of spasticity (Figures 2b and 3a). In the first phase (0–4 weeks after stroke), we observed a relatively small, yet significant, difference in the RDDs of sham-operated and stroke mice. However, in the second phase (4–8 weeks after stroke), the H-reflex in stroke mice was not highly depressed by 5-Hz stimulation. Moreover, the number

of c-Fos-positive cells was elevated in the period from 0 to 4 weeks after stroke but gradually decreased during 4–8 weeks after stroke (Figures 5a and b). It can thus be hypothesized that plasticity at the spinal and neuromuscular levels may occur, for instance, the number of motoneuron synapses may increase[29] or the development of motoneuron axonal arbors may be enhanced.[30] These changes could account for the significant difference in RDDs that we observed during the second phase compared with the first phase.

Our results demonstrated that the number of c-Fos-positive motoneurons in for both affected and unaffected motoneurons was significantly elevated in stroke mice compared with sham-operated mice (Figures 4d–g). Previous studies have also reported neuronal plasticity in unaffected neurons and contra-lesioned corticospinal axons after cortical injury.[31,32] One reason for plasticity in the unaffected side may be injury of neurons in the rostral and caudal forelimb motor areas that disynaptically project to unaffected spinal cord motoneurons. In other words, motor and supplemental motor cortical areas project to both sides of the brainstem but especially to the ipsilateral brainstem.[33,34] As brainstem neurons project to the spinal cord, bilateral spinal cord motoneurons are indirectly influenced. However, H-reflex RDDs in unaffected motoneurons were not significantly weakened in stroke mice compared with sham-operated mice except at 1 and 8 weeks post stroke (Figure 2d). The reason why H-reflex RDDs in unaffected side post-stroke mice were not significantly weakened compared with sham-operated mice is unclear.

With regard to spinal cord injury, it was previously hypothesized that one of the main mechanisms of spasticity was increased motoneuron excitability.[11,35,36] In our mouse spasticity model, we examined motoneuron excitability by assessing c-fos mRNA expression and c-Fos immuno-reactivity in motoneurons, and we found that levels of both were significantly increased in the affected spinal cord after stroke. Boulenguez *et al.*[11] recently reported that one of the reasons for motoneuron excitability after spinal cord injury is down-regulation of the potassium chloride cotransporter KCC2; when this occurs, inhibitory $GABA_A$ and glycine receptors switch from depolarizing to hyperpolarizing actions of GABA and glycine, respectively, resulting in low intracellular Cl^- concentrations.[11,37] Moreover, a previous study reports as other spasticity mechanism that the serotonergic 5-HT2C receptor changes constitutive active after spinal cord injury.[38] Furthermore, patients with multiple sclerosis, which is an autoimmune disease, also exhibit spasticity. These lines of evidence indicate that several other mechanisms may contribute to post-stroke spasticity.

We used H-reflex RDD, which is believed to cause both presynaptic and motoneuron excitability, as a measure of spasticity.[14,17,39,40] In previous studies, H-reflex RDD was used as a measure of spasticity, we also observed significance weakened H-reflex RDDs at 4 weeks after spinal cord injury (data not shown).[1,9,11] It is known that repetitive firing of synapses leads to a temporary decrease in synaptic strength,[41] possibly due to a decrease in presynaptic Ca^{2+} current,[42] vesicle depletion,[41] postsynaptic receptor desensitization,[43,44] activity-dependent decrease in neurotransmitter release probability[45,46] and action potential conduction failure in the postsynaptic neuron.
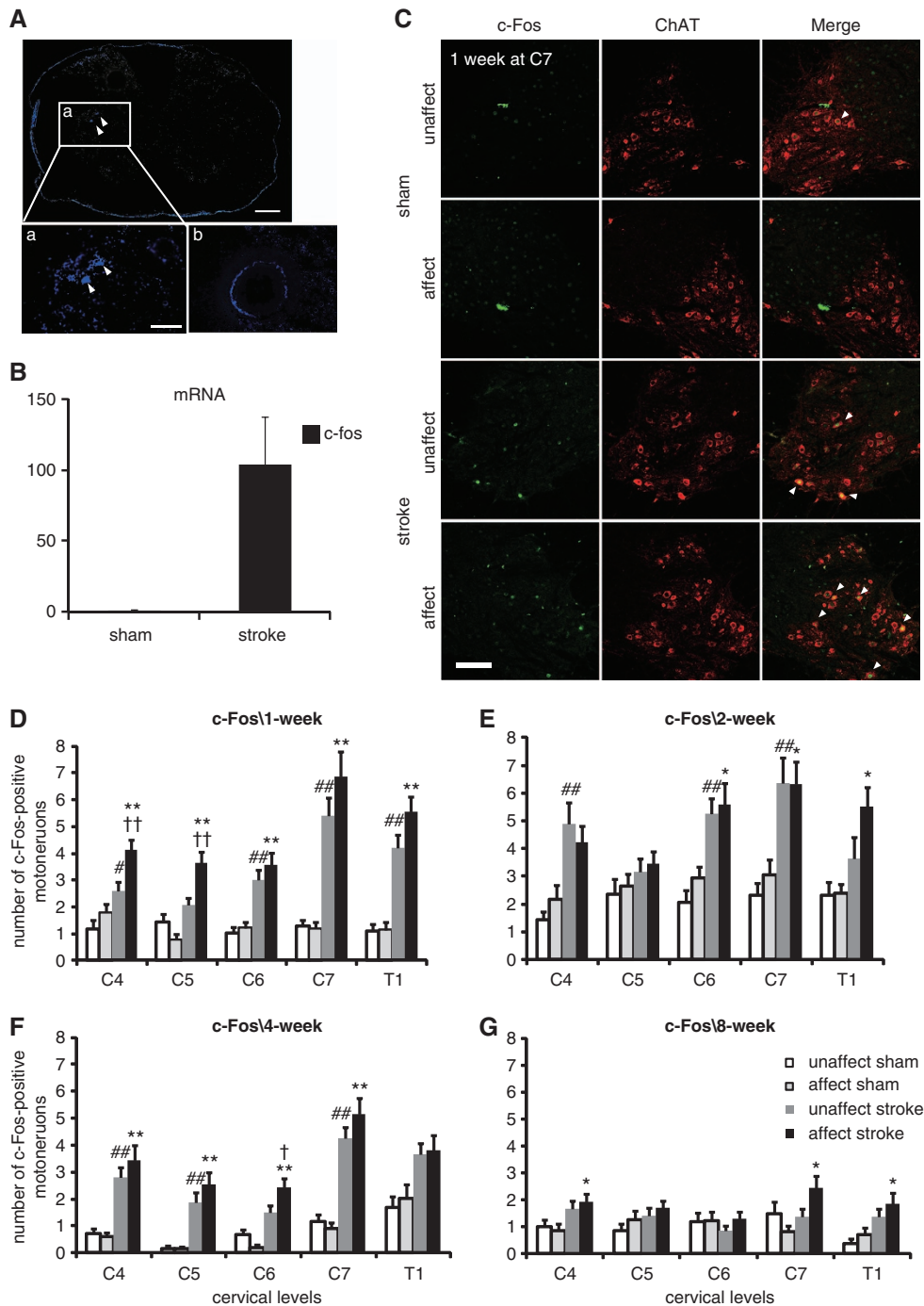
Figure 4 Increased c-fos mRNA levels in affected motoneurons after stroke. (**A**) Cross-sections of the spinal cord at C7. The motoneurons were labeled with the retrograde tracer True Blue to isolate the motoneurons with LMD. Bar = 200 μm. (a) Magnified view of the square in panel (**A**). The arrowheads indicate motoneurons labeled with True Blue. (b) Labeled motoneurons were isolated by LMD. (a and b): Bar = 100 μm. (**B**) Quantification of c-fos mRNA expression in the affected motoneurons 1 week after stroke (by RT-PCR). The fold change in c-fos mRNA expression in the stroke group relative to the sham-operated group is presented as the mean ± S.E.M. ($n = 4$ for sham-operated mice and $n = 3$ for stroke mice, approximately 50 motoneurons for each animal; **$P < 0.01$ by Mann–Whitney U-test). (**C**) At 1 week after stroke, c-Fos-positive motoneurons in C7 increased in both the affected and unaffected sides of stroke mice compared with the respective side of sham-operated mice. Bars = 100 μm. (**D–G**) Quantitative analyses of the number of c-Fos-ChAT double-positive motoneurons (arrowhead) in affected and unaffected spinal cord levels (C4–T1) in sham-operated and stroke mice at 1, 2, 4, and 8 weeks after stroke. *$P < 0.05$, **$P < 0.01$ between sham-operated and stroke mice on the affected side; #$P < 0.05$, ##$P < 0.01$ between sham-operated and stroke mice on the unaffected side; †$P < 0.05$, ††$P < 0.01$ between unaffected and affected sides in stroke mice (one-way ANOVAs followed by Tukey–Kramer tests)

H-reflex RDD is useful for determining changes in spinal cord function after injury.[10,11,47–49] In our model, motoneuron excitability, an important spastic symptom, was confirmed by changes in H-reflex RDD and c-Fos expression, which highlights the potential of using this protocol to model post-stroke spasticity.
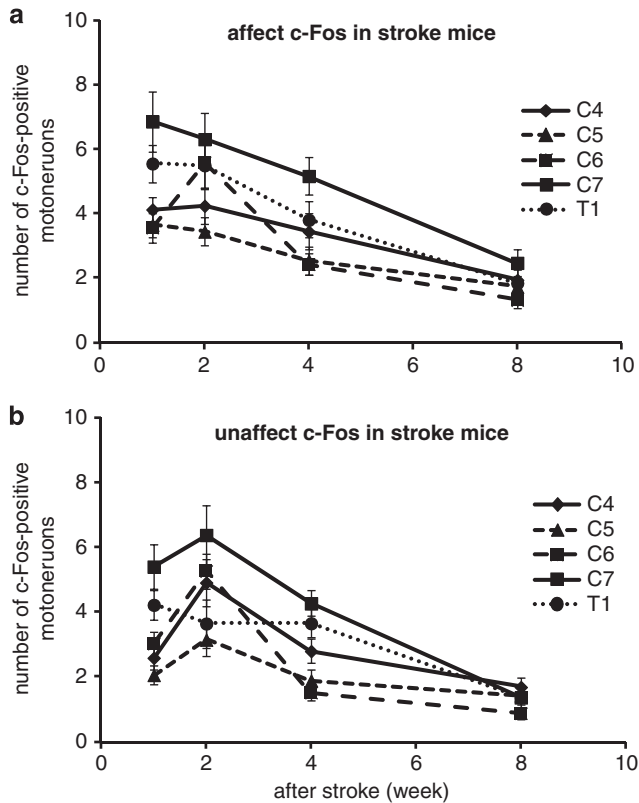
Figure 5 Changes in the number of c-Fos-positive motoneurons in (a) affected and (b) unaffected sides of the spinal cord from 1 to 8 weeks after stroke. Data are represented as mean ± S.E.M. (Spearman's correlation coefficient by rank test)

Figure 6 H-reflex RDDs 1 week post stroke in mice treated with baclofen. H-reflex RDD in (a) baclofen- or vehicle-injected intact mice or (b) 1-week stroke mice. Response data are expressed as percentages relative to the mean responses at 0.1 Hz in the same series of measurements. Data are represented as mean ± S.E.M. (**$P < 0.01$, one-way ANOVA followed by Tukey–Kramer tests)

Although there are other parameters for assessing spasticity in patients with spinal cord injury and stroke, such as the modified Ashworth scale scored by the degree of muscle tone, these measurements cannot be used in animal models.[50–53] Apparent spastic behavior was not detected in our model, which may be due to the lack of an appropriate parameter for assessing spastic behavior in rodents. Given that we did not clearly observe spastic behavior, we are currently trying to detect abnormal muscle contractions or neuromuscular junction changes using morphological analyses. These parameters could be used as spasticity markers in the future. Our model of spasticity after stroke can potentially help elucidate spasticity pathophysiology, which could aid the development of pharmacological and rehabilitation treatments.

Materials and Methods

Animals. Adult male C57BL/6J mice (20–30 g, 8–10-weeks old, Japan SLC, Inc., Shizuoka, Japan) were housed in standard cages with food and water *ad libitum* and maintained under a 12-h light-dark cycle. All procedures were approved by the Nagoya University Guidelines for the Care and Use of Laboratory Animals.

Photothrombotic cortical lesion. Focal cortical ischemia was induced by cortical microvessel photothrombosis, as described previously.[21,22] Mice were anesthetized with intraperitoneal sodium pentobarbital (Somnopentyl, 50 mg/kg body weight; Kyouritu Seiyaku, Tokyo, Japan) and then individually placed on a stereotaxic frame for surgery. Rose Bengal (30 mg/kg body weight; Sigma-Aldrich, St. Louis, MO, USA) was injected into the tail vein 5 min before illumination, and the skull was exposed via a midline incision of the skin. Focal illumination of the rostral and caudal forelimb motor areas (+ 3.0-mm to − 1.5-mm anteroposterior,
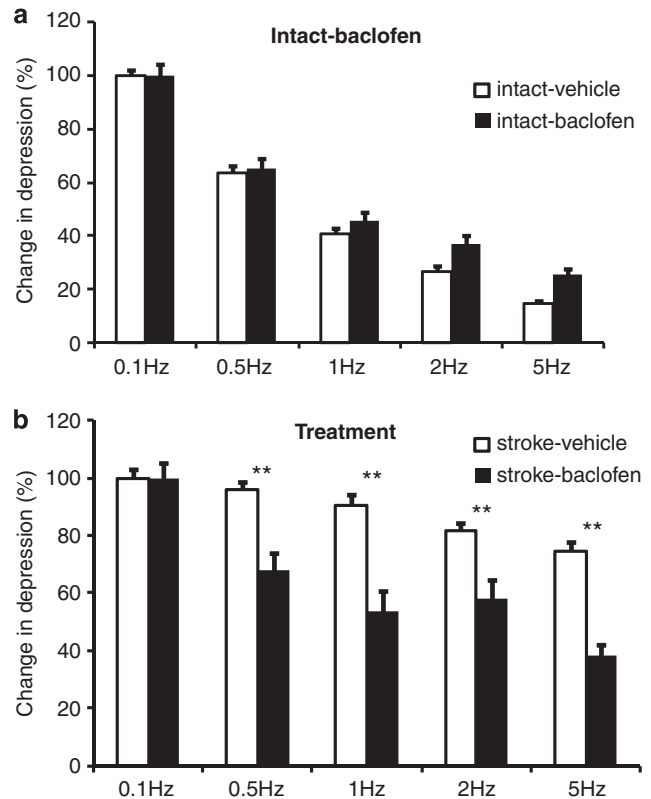
3.0–0.5-mm lateral to bregma) (Figures 7a and b) was carried out with a cold light source (KL1500LCD, Zeiss, Oberkochen, Germany), with a 4.5-mm aperture[54] through the intact skull; the brain was illuminated for 15 min.[22] The scalp was then sutured, and the mice were allowed to recover. Control mice either received the same injection of Rose Bengal without illumination ($n = 10$) or were photostimulated after an intravenous injection of 0.9% NaCl solution ($n = 4$).

Electrophysiological recordings. We modified a previously described method to use the RDD of the H-reflex as a measurement of spastic symptoms[11,55] Mice were anesthetized with ketamine (200 mg/kg, CS Pharmacology Co., Ltd., Aichi, Japan), which is widely used during H-reflex recordings (Figure 8a). If required, an additional 25% dose of anesthesia was given every 30 min to suppress whisker tremors or voluntary movements. The forelimbs and hindlimbs of the mice were fixed on a plate with a plastic tape, and their positions were controlled to avoid unnecessary pressure and stretch that could affect the electrophysiological responses of the muscles and nerves (Figure 8b). To maintain the body temperature, the plate was placed on a warm pad maintained at approximately 37 °C. We transcutaneously inserted a pair of stainless needle electrodes (EKA2-1508, Bioresearch Center Corporation, Aichi, Japan) fixed with micromanipulator (SM-15, NARISHIGE, Tokyo, Japan) into nerve bundles, including the ulnar nerve and stimulated with a stimulator (1–3 mA in 0.1 mA increments, SEN—7103, Nihon Kohden Corporation, Aichi, Japan). For recording, a pair of stainless needle electrodes fixed with manipulator (YOU-2, NARISHIGE) was transcutaneously placed into the abductor digiti minimi muscles and obtained recordings with an amplifier (High pass: 0.1, SS-201J, Nihon Kohden Corporation) and an A/D converter (Low pass: 1 kHz, PowerLab, ADInstruments Japan Inc., Aichi, Japan). We initially stimulated the nerves for 0.2 ms at 0.1 Hz and then gradually increased the current intensity; in this way, we were able to determine the intensity necessary to obtain a maximal H-reflex. Following this, we used an intensity of 23 stimulation trains at 0.1, 0.5, 1, 2, and 5 Hz, with 2-min intervals
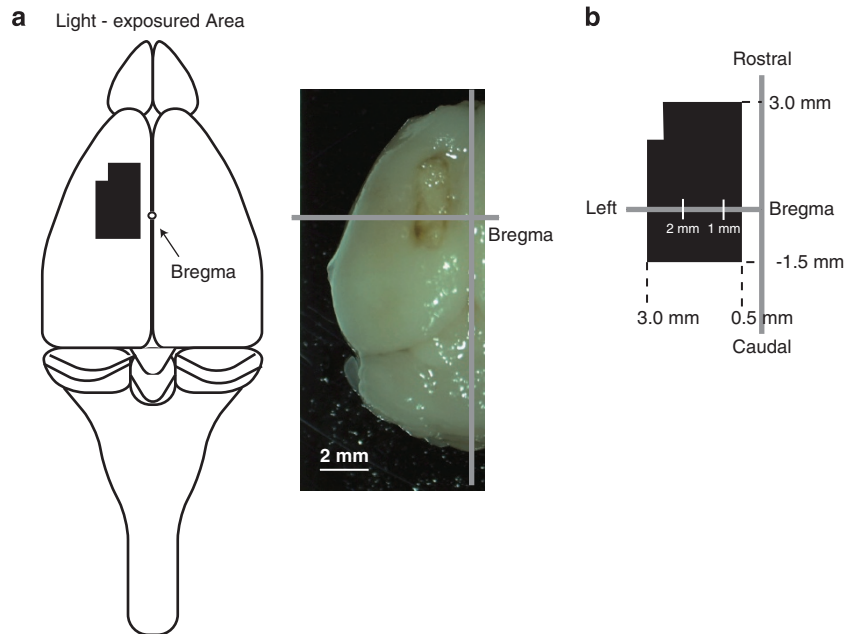
Figure 7 Stroke lesion areas in the left rostral and caudal forelimb motor areas. (**a**) Image of a photochemically injured cortex. (**b**) The light beam was exposed to the brain at the following coordinates: $+3$-mm to -1.5-mm antero-posterior and from 0.5-mm to 3.0-mm lateral to the left of bregma in the rostral and caudal forelimb areas
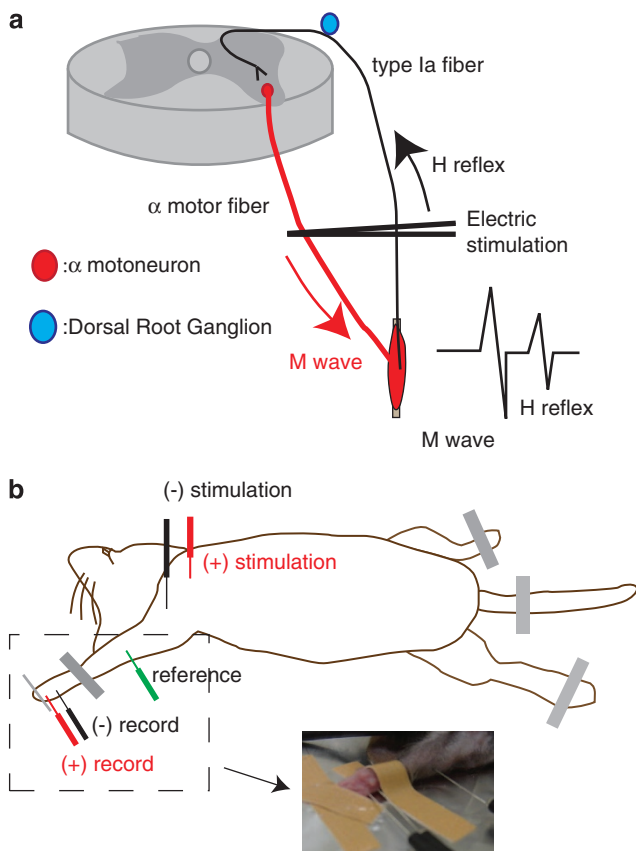
Figure 8 (**a**) Illustration of the M wave and H-reflex and (**b**) the method used to measure the H-reflex in the abductor digiti minimi muscle of the mouse

between each train, to measure the RDD. To determine the RDD at different frequencies, we discarded the responses to the first three stimulations that were necessary for depression to occur and expressed all of the remaining responses as percentages relative to the mean response at 0.1 Hz in the same series of measurements.

LMD and real time RT-PCR preparation. To obtain samples of the affected motoneurons in the abductor muscles of the little finger, we labeled the motoneurons with the retrograde tracer 1% True Blue (T5891, Sigma-Aldrich); the tracer was diluted with water and injected into the right abductor digiti minimi muscle. The spinal cords (C6 to Th1) were removed from both sham-operated and stroke mice, and the collected samples were cut into 30-μm sections with a cryostat. The labeled motoneurons were collected with an LMD system (LMD 6500, Leica Microsystems K. K., Tokyo, Japan; Figure 3). After total RNA was isolated from the obtained neurons, the RNAs were transcribed to cDNA and amplified with a Prelude and Ovation WTA system (PicoSL WTA system V2, NuGEN Technologies, Inc., San Carlos, CA, USA).

Quantitative analysis of real-time RT-PCR. Quantitative analysis for real-time RT-PCR was performed using an oligonucleotide primer sets that corresponded to the cDNA sequences of c-fos (forward: 5′-GGGAGGACCTTACC TGTTCGT-3′, reverse: 5′-GGATGCTTGCAAGTCCTTGAG-3′), ChAT (forward: 5′-ACATATGATGACAGGCAACAAGAAG-3′, reverse: 5′-GGGAGCAGGGAGTTC ACTCA-3′), and glyceraldehyde-3-phosphate dehydrogenase (GAPDH, forward: 5′-GGGCTGGCATTGCTCTCA-3′, reverse: 5′-TGTAGCCGTATTCATTGTCATA CCA-3′). We used the ABI StepOne Plus system (Applied Biosystems, Life Technologies Corporation, Grand Island, NY, USA). The reaction mixture (10 μl), containing 5 μl SYBR Green real-time PCR master mix (THUNDERBIRD SYBR q PCR Mix, Toyobo Co., Ltd., Osaka, Japan), 0.2 μl of both the sense and antisense primers (10 μM), and 1 μl cDNA sample (10 ng), was preheated at 95 °C for 3 min and then treated with 40 cycles of amplification (denaturation at 95 °C for 15 s and annealing and extension at 60 °C for 1 min). The relative intensity against GAPDH and the fold-change relative to the controls were calculated with $\Delta\Delta$CT analyses. mRNA levels of ChAT, a motoneuron differentiation marker, were also measured.

c-Fos immunohistochemical analysis. At 1, 2, 4, and 8 weeks after stroke, some mice ($n=3$ each) were deeply anesthetized and then transcardially perfused with 4% paraformaldehyde (PFA) dissolved in 0.1 M phosphate buffer. The spinal cord from the cervical to the upper thoracic region was removed and fixed in 4% PFA at 4 °C overnight and then cryoprotected in 30% sucrose for 3 days. The tissues were embedded in optimal cutting temperature compound (Tissue-Tek, SAKURA Finetek, Tokyo, Japan) and stored at -80 °C. Coronal sections of the spine (20–30-μm thick) were prepared with a cryostat.

Sections were then stored in the cryoprotectant ethylene glycol at $-20\,^{\circ}\mathrm{C}$ until the time of use. Briefly, we removed tissue sections from the cryoprotectant and washed them in phosphate-buffered saline (PBS). We then pre-incubated the tissue in blocking buffer (5% normal bovine serum and 0.25% Triton X-100 in PBS) for 1 h at $25\,^{\circ}\mathrm{C}$, followed by incubation with a c-Fos antibody (sc-52, 1 : 1000, Santa Cruz Biotechnology, Santa Cruz, CA, USA) and ChAT antibody (AB144P, 1 : 500, Millipore, Billerica, MA, USA) in blocking buffer for 24 h at room temperature. After washing in PBS, the tissue was incubated for 1 h in a solution containing Alexa Fluor 488 and 568 conjugated to donkey anti-rabbit (1 : 1000) and donkey anti-goat (1 : 500) immunoglobulin G, respectively (Molecular Probes, Invitrogen, Carlsbad, CA, USA). The sections were counterstained with DAPI (4′,6-diamidino-2-phenylindole). All the sections were examined by fluorescence microscopy (magnification, $\times100$, BZ-9000 BIOREVO, KEYENCE, Osaka, Japan) or confocal laser scanning microscopy (magnification, $\times100$, A1Rsi, Nikon, Tokyo, Japan). For quantification, c-Fos-positive motoneurons, stained with ChAT, were counted in 10 cross-sections per cervical and upper thoracic level (C4–T1).

Baclofen treatment. This blind experiment of intraperitoneal injection of baclofen was performed using a modified procedure as previously described.[27] We confirmed the weakened RDDs in the abductor digiti minimi muscle at 3 days after stroke. The stroke mice were intraperitoneally injected with baclofen ($n = 5$, 9 mg/kg weight, diluted with 0.9% NaCl, Sigma-Aldrich) or 0.9% NaCl ($n = 4$) as vehicle at 7 days post stroke. H-reflex RDDs of injected mice were measured 90 min after the injection. To assess the effect of baclofen in intact mice, we also measured RDDs in baclofen-injected intact mice.

Statistical analyses. Group measurements are expressed as mean $\pm$ S.E.M. H-reflex RDDs were determined as a measurement of spasticity and analyzed with one-way analysis of variance (ANOVA) and Tukey–Kramer Tests. For real-time RT-PCR analysis, we used Mann–Whitney U-tests and Student's t-tests to compare data obtained from the sham-operated and stroke groups. For c-Fos immunohistochemical analysis, we used ANOVA, Tukey–Kramer tests, and Spearman's correlation coefficient by rank test. P-values <0.05 were considered significant.

Conflict of Interest

The authors declare no conflict of interest.

1. Nielsen J, Petersen N, Crone C. Changes in transmission across synapses of Ia afferents in spastic patients. Brain 1995; 118(Pt 4): 995–1004.
2. Dietz V, Sinkjaer T. Spastic movement disorder: impaired reflex function and altered muscle mechanics. Lancet Neurol 2007; 6: 725–733.
3. Sommerfeld DK, Eek EU, Svensson AK, Holmqvist LW, von Arbin MH. Spasticity after stroke: its occurrence and association with motor impairments and activity limitations. Stroke 2004; 35: 134–139.
4. Sommerfeld DK, Gripenstedt U, Welmer AK. Spasticity after stroke: an overview of prevalence, test instruments, and treatments. Am J Phys Med Rehabil 2012; 91: 814–820.
5. Koganemaru S, Mima T, Thabit MN, Ikkaku T, Shimada K, Kanematsu M et al. Recovery of upper-limb function due to enhanced use-dependent plasticity in chronic stroke patients. Brain 2010; 133: 3373–3384.
6. Urban PP, Wolf T, Uebele M, Marx JJ, Vogt T, Stoeter P et al. Occurence and clinical predictors of spasticity after ischemic stroke. Stroke 2010; 41: 2016–2020.
7. Nielsen JB, Crone C, Hultborn H. The spinal pathophysiology of spasticity—from a basic science point of view. Acta Physiol (Oxf) 2007; 189: 171–180.
8. Emmanuel Pierrot-Deseilligny DB. The Circuitry of the Human Spinal Cord: Spinal and Corticospinal Mechanisms and Movement. Cambridge University Press, 2012.
9. Lamy JC, Wargon I, Mazevet D, Ghanim Z, Pradat-Diehl P, Katz R. Impaired efficacy of spinal presynaptic mechanisms in spastic stroke patients. Brain 2009; 132: 734–748.
10. Higashi T, Funase K, Kusano K, Tabira T, Harada N, Sakakibara A et al. Motoneuron pool excitability of hemiplegic patients: assessing recovery stages by using H-reflex and M response. Arch Phys Med Rehabil 2001; 82: 1604–1610.
11. Boulenguez P, Liabeuf S, Bos R, Bras H, Jean-Xavier C, Brocard C et al. Down-regulation of the potassium-chloride cotransporter KCC2 contributes to spasticity after spinal cord injury. Nat Med 2010; 16: 302–307.
12. Malhotra S, Pandyan AD, Rosewilliam S, Roffe C, Hermens H. Spasticity and contractures at the wrist after stroke: time course of development and their association with functional recovery of the upper limb. Clin Rehabil 2011; 25: 184–191.
13. Lukacs M. F wave measurements detecting changes in motor neuron excitability after ischaemic stroke. Electromyogr Clin Neurophysiol 2007; 47: 109–115.
14. Mottram CJ, Wallace CL, Chikando CN, Rymer WZ. Origins of spontaneous firing of motor units in the spastic-paretic biceps brachii muscle of stroke survivors. J Neurophysiol 2010; 104: 3168–3179.
15. Murase N, Duque J, Mazzocchio R, Cohen LG. Influence of interhemispheric interactions on motor function in chronic stroke. Ann Neurol 2004; 55: 400–409.
16. Mazzocchio R, Rossi A. Involvement of spinal recurrent inhibition in spasticity. Further insight into the regulation of Renshaw cell activity. Brain 1997; 120(Pt 6): 991–1003.
17. McPherson JG, Ellis MD, Heckman CJ, Dewald JP. Evidence for increased activation of persistent inward currents in individuals with chronic hemiparetic stroke. J Neurophysiol 2008; 100: 3236–3243.
18. Fulton JF, Kennard MA. A study of flaccid and spastic paralyses produced by lesions of the cerebral cortex in primates. Res Pubublication Assoc Ment Dis 1934; 13: 158–210.
19. Rouiller EM, Moret V, Liang F. Comparison of the connectional properties of the two forelimb areas of the rat sensorimotor cortex: support for the presence of a premotor or supplementary motor cortical area. Somatosens Mot Res 1993; 10: 269–289.
20. Paz JT, Christian CA, Parada I, Prince DA, Huguenard JR. Focal cortical infarcts alter intrinsic excitability and synaptic excitation in the reticular thalamic nucleus. J Neurosci 2010; 30: 5465–5479.
21. Lee JK, Kim JE, Sivula M, Strittmatter SM. Nogo receptor antagonism promotes stroke recovery by enhancing axonal plasticity. J Neurosci 2004; 24: 6209–6217.
22. Clarkson AN, Huang BS, Macisaac SE, Mody I, Carmichael ST. Reducing excessive GABA-mediated tonic inhibition promotes functional recovery after stroke. Nature 2010; 468: 305–309.
23. Mazevet D, Meunier S, Pradat-Diehl P, Marchand-Pauvert V, Pierrot-Deseilligny E. Changes in propriospinally mediated excitation of upper limb motoneurons in stroke patients. Brain 2003; 126: 988–1000.
24. Ueno M, Yamashita T. Kinematic analyses reveal impaired locomotion following injury of the motor cortex in mice. Exp Neurol 2011; 230: 280–290.
25. Flavell SW, Greenberg ME. Signaling mechanisms linking neuronal activity to gene expression and plasticity of the nervous system. Annu Rev Neurosci 2008; 31: 563–590.
26. Nomura S, Kagawa Y, Kida H, Maruta Y, Imoto H, Fujii M et al. Effects of intrathecal baclofen therapy on motor and cognitive functions in a rat model of cerebral palsy. J Neurosurg Pediatr 2012; 9: 209–215.
27. Pravetoni M, Wickman K. Behavioral characterization of mice lacking GIRK/Kir3 channel subunits. Genes Brain Behav 2008; 7: 523–531.
28. Bhakta BB. Management of spasticity in stroke. Br Med Bull 2000; 56: 476–485.
29. Tan AM, Chakrabarty S, Kimura H, Martin JH. Selective corticospinal tract injury in the rat induces primary afferent fiber sprouting in the spinal cord and hyperreflexia. J Neurosci 2012; 32: 12896–12908.
30. Nicaise C, Hala TJ, Frank DM, Parker JL, Authelet M, Leroy K et al. Phrenic motor neuron degeneration compromises phrenic axonal circuitry and diaphragm activity in a unilateral cervical contusion model of spinal cord injury. Exp Neurol 2012; 235: 539–552.
31. Lee S, Ueno M, Yamashita T. Axonal remodeling for motor recovery after traumatic brain injury requires downregulation of gamma-aminobutyric acid signaling. Cell Death Dis 2011; 2: e133.
32. Ueno M, Hayano Y, Nakagawa H, Yamashita T. Intraspinal rewiring of the corticospinal tract requires target-derived brain-derived neurotrophic factor and compensates lost function after brain injury. Brain 2012; 135: 1253–1267.
33. Keizer K, Kuypers HG. Distribution of corticospinal neurons with collaterals to the lower brain stem reticular formation in monkey (Macaca fascicularis). Exp Brain Res 1989; 74: 311–318.
34. Matsuyama K, Drew T. Organization of the projections from the pericruciate cortex to the pontomedullary brainstem of the cat: a study using the anterograde tracer Phaseolus vulgaris-leucoagglutinin. J Comp Neurol 1997; 389: 617–641.
35. Boulenguez P, Vinay L. Strategies to restore motor functions after spinal cord injury. Curr Opin Neurobiol 2009; 19: 587–600.
36. Li Y, Gorassini MA, Bennett DJ. Role of persistent sodium and calcium currents in motoneuron firing and spasticity in chronic spinal rats. J Neurophysiol 2004; 91: 767–783.
37. Payne JA, Rivera C, Voipio J, Kaila K. Cation-chloride co-transporters in neuronal communication, development and trauma. Trends Neurosci 2003; 26: 199–206.
38. Murray KC, Nakae A, Stephens MJ, Rank M, D'Amico J, Harvey PJ et al. Recovery of motoneuron and locomotor function after spinal cord injury depends on constitutive activity in 5-HT2C receptors. Nat Med 2010; 16: 694–700.
39. Guissard N, Duchateau J, Hainaut K. Mechanisms of decreased motoneurone excitation during passive muscle stretching. Exp Brain Res 2001; 137: 163–169.
40. Hultborn H, Illert M, Nielsen J, Paul A, Ballegaard M, Wiese H. On the mechanism of the post-activation depression of the H-reflex in human subjects. Exp Brain Res 1996; 108: 450–462.
41. Foster KA, Regehr WG. Variance-mean analysis in the presence of a rapid antagonist indicates vesicle depletion underlies depression at the climbing fiber synapse. Neuron 2004; 43: 119–131.

42. Xu J, He L, Wu LG. Role of Ca(2 +) channels in short-term synaptic plasticity. *Curr Opin Neurobiol* 2007; **17**: 352–359.

43. Chen C, Blitz DM, Regehr WG. Contributions of receptor desensitization and saturation to plasticity at the retinogeniculate synapse. *Neuron* 2002; **33**: 779–788.

44. Wong AY, Graham BP, Billups B, Forsythe ID. Distinguishing between presynaptic and postsynaptic mechanisms of short-term depression during action potential trains. *J Neurosci* 2003; **23**: 4868–4877.

45. Sakaba T, Neher E. Quantitative relationship between transmitter release and calcium current at the calyx of held synapse. *J Neurosci* 2001; **21**: 462–476.

46. Wu LG, Borst JG. The reduced release probability of releasable vesicles during recovery from short-term synaptic depression. *Neuron* 1999; **23**: 821–832.

47. Hosoido T, Goto M, Sano Y, Mori F, Nakajima K, Morita F *et al.* Hoffmann reflex in a rat bipedal walking model. *Neurosci Lett* 2011; **505**: 263–267.

48. Thompson FJ, Reier PJ, Lucas CC, Parmer R. Altered patterns of reflex excitability subsequent to contusion injury of the rat spinal cord. *J Neurophysiol* 1992; **68**: 1473–1486.

49. Grey MJ, Klinge K, Crone C, Lorentzen J, Biering-Sorensen F, Ravnborg M *et al.* Post-activation depression of soleus stretch reflexes in healthy and spastic humans. *Exp Brain Res* 2008; **185**: 189–197.

50. Bennett DJ, Gorassini M, Fouad K, Sanelli L, Han Y, Cheng J. Spasticity in rats with sacral spinal cord injury. *J Neurotrauma* 1999; **16**: 69–84.

51. Murray KC, Stephens MJ, Ballou EW, Heckman CJ, Bennett DJ. Motoneuron excitability and muscle spasms are regulated by 5-HT2B and 5-HT2C receptor activity. *J Neurophysiol* 2011; **105**: 731–748.

52. Boutilier G, Sawatzky BJ, Grant C, Wiefelspuett S, Finlayson H. Spasticity changes in SCI following a dynamic standing program using the Segway. *Spinal Cord* 2012; **50**: 595–598.

53. Haas BM, Bergstrom E, Jamous A, Bennie A. The inter rater reliability of the original and of the modified Ashworth scale for the assessment of spasticity in patients with spinal cord injury. *Spinal Cord* 1996; **34**: 560–564.

54. Tennant KA, Adkins DL, Donlan NA, Asay AL, Thomas N, Kleim JA *et al.* The organization of the forelimb representation of the C57BL/6 mouse motor cortex as defined by intracortical microstimulation and cytoarchitecture. *Cereb Cortex* 2011; **21**: 865–876.

55. Navarro X, Verdu E, Buti M. Comparison of regenerative and reinnervating capabilities of different functional types of nerve fibers. *Exp Neurol* 1994; **129**: 217–224.